2021

# A Modeling Approach to Characterize the Demand Flexibility of the Air Distribution System in Commercial Buildings

Elvin Vindel
*Carnegie Mellon University*, evindel@andrew.cmu.edu

Mario Berges

Burcu Akinci

# A Modeling Approach to Characterize the Demand Flexibility of the Air Distribution System in Commercial Buildings

Elvin VINDEL*, Mario BERGES, Burcu AKINCI

Carnegie Mellon University, Department of Civil and Environmental Engineering
Pittsburgh, Pennsylvania, USA
Email: {evindel, marioberges, bakinci}@cmu.edu

* Corresponding Author

## ABSTRACT

Commercial VAV systems have been a studied as potential flexible power consumption resources to provide these services. A significant limitation is the development of control oriented models for these systems that accurately control power consumption across timescales. To this end, we develop a modeling approach that characterizes the demand flexibility of the air distribution system in commercial buildings. The model maps all feasible terminal zone damper configurations to power consumption by identifying a system resistance model connected to a pressure-flow model of the supply fan. Under this model structure, the operational range of an installed system can be quantitatively bounded by the extreme resistance curves the air distribution system encounters. We also propose a simplified control algorithm that leverages this model structure to emulate a demand flexibility event. We validate this approach by calibrating a model in an experimental testbed and additionally testing the results in a simulation environment. A brief discussion of important properties and observations that can be derived from this approach as well as avenues for improvements is presented.

## 1. INTRODUCTION

The sustainable integration of large shares of renewable energy in the power grid requires more sources of flexibility to balance the grid's operation (Ulbig & Andersson, 2015). Buildings have a valuable untapped potential to provide some of this flexibility through reliability-based grid services (Neukomm, Nubbe, & Fares, 2019). In particular, commercial VAV systems have received attention due to their significant energy consumption and pre-existing automation capabilities (Goddard, Klose, & Backhaus, 2014). Recent research has demonstrated, through a variety of control algorithms, that the thermal capacity of zones can allow for flexible power consumption. The majority of this research has focused on simulation models that characterize demand flexibility uniquely as a property of the building's envelope and thermal mass (Kathirgamanathan, De Rosa, Mangina, & Finn, 2021). However, to accurately model the effect of advanced control strategies on power consumption, a more detailed model of the building mechanical system with high predictive accuracy is necessary (Yin, Kiliccote, & Piette, 2016).Within the scope of commercial VAV systems, air distribution system modeling has been labeled a deficient core modeling capability in modern building energy modeling (Roth & Reyna, 2020). Moreover, recent studies highlight the limitations of existing modeling approaches in supporting experimental observations, particularly for complex demand flexibility events (MacDonald, Vrettos, & Callaway, 2020). This is a challenge because the deployment of this technology for advanced grid services requires performance guarantees in predicting the duration, ramp time, and magnitude of power deviations.

Due to the relatively large impact of fans on energy consumption in buildings served by large central multizone HVAC systems (20 to 80% according to (ASHRAE, 2016)), our goal is to develop a model for the supply fan in a VAV system so as to accurately control and characterize its power consumption for more stringent demand flexibility applications (i.e. contingency reserves, regulation, ramping, etc.). Based on the common structure of most VAV systems, and shared control architecture, several control inputs are candidates to modify the power consumption of the supply fan. These control inputs, and their respective control loops can be visualized in Figure 1. At the AHU level, two control inputs can be actuated through the fan controller: the rotational speed of the fan, (Macdonald, Kiliccote, Boch, Chen, & Nawy, 2014), and the static pressure setpoint, $\hat{p}$, (Adetola et al., 2018). Although high accuracy models have been developed with these inputs, it is possible to cause undesirable effects on downstream components (Goddard et al., 2014). At the zone level, three control inputs can be modified having an indirect effect on fan power consumption. Figure 1 shows

the controls of one of such zones; multizone VAV systems have $N$ such zone subsystems. Temperature setpoint reset, $\hat{\mathbf{T}}$, is commonly used in practice and in literature due to its simplicity (Goddard et al., 2014). However, given that several control loops separate this input and the AHU, it has been shown to have a complex and sometimes negligible effect on power (Keskar, Anderson, Johnson, Hiskens, & Mathieu, 2019). Zone airflow setpoint, $\hat{\mathbf{q}}$, is a popular choice connecting to both the zone thermal dynamics and power through the fan laws (Wang, Huang, Wu, & Lu, 2020). This modeling approach is implemented at the expense of simplifying the pressure dynamics of the fan-duct system. To accurately control power consumption, a model should include both the pressure and flow dimensions (known as the operating point) (Stein & Hydeman, 2004). Zone damper positions, $\boldsymbol{\theta}$, actively influence the pressure dynamics of the duct network. In most VAV systems, the supply fan is a pressure-controlled device, meaning that zone dampers are the unfiltered connection between the control inputs at the zone level and the supply fan. This property makes damper position control stand out as a control input choice to modify the fan power consumption.

Models that focus on the relation between damper positions and the pressure dynamics are commonly used for static pressure reset analysis. A statistical model was developed to predict the energy savings from pressure reset strategies using historical building automation system (BAS) data (Tukur & Hallinan, 2017). More recently, a mathematical model coupled with newer machine learning techniques was developed to find the optimal reset strategy for energy savings (Jing et al., 2019). Although these approaches capture the pressure-flow dynamics, they have not been applied to the context of control for demand flexibility. Nonetheless, because of the modeling need described above, recent works have revisited models that include damper position control, as it is a significant factor in the effectiveness of demand flexibility strategies (Blum & Norford, 2014). A detailed model was developed for supply fan power consumption that include the pressure-flow dynamics (Hydeman, Taylor, Stein, Kolderup, & Hong, 2003). Although this model characterizes the operational range of the system, a connection to zone damper positions is not explored. A generic polynomial multi-regression model was developed by taking as inputs pressure, flow, and damper positions to predict fan energy consumption (Dong et al., 2019). The model's predictive capabilities were evaluated, but the authors do not elaborate on how this model can be used for fan control. Pertinent to our work, a single-zone mathematical model from damper positions, and their pressure drop characteristics, to fan power was developed (Raisoni, Raman, Barooah, Munk, & Im, 2018). Due to the model complexity, this approach required the identification of 8 parameters per zone, scaling linearly with the number of zones. Furthermore, the identification process required targeted experiments beyond nominal operation making it unclear whether this approach is generalizable or scalable.

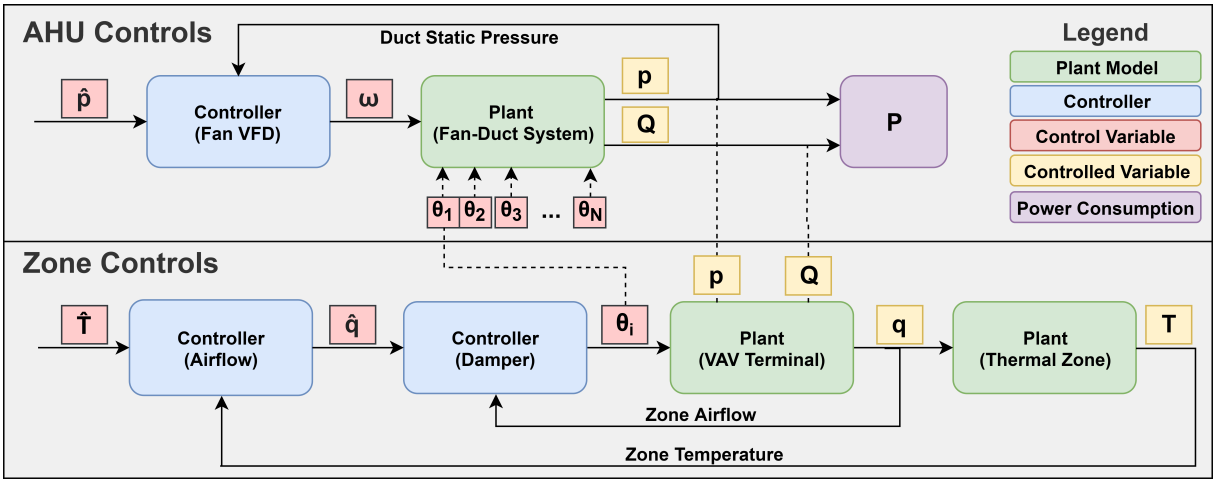


**Figure 1:** Diagram of common control architecture in multizone VAV systems

From prior work we observe three areas for improvement. First, the proposed model structures do not characterize the operational range that can be actuated for an installed system to modify fan power. Defining these bounds provides a quantitative measure of the technical capability of the system to modify its power consumption (i.e. demand flexibility). Our approach proposes using the extreme system resistance curves as a method to characterize the range of power consumption. Second, current work is primarily validated for predictive capabilities, and does not elaborate on the effect of dynamic control inputs on power consumption. We propose the use of two low complexity models (system resistance and pressure-flow) to map the relation between terminal damper positions and fan power consumption. In

addition, we present an algorithm that uses this structure to control the system resistance using damper position inputs and predicting the future operating point, hence the power consumption. Under this framework, the dynamics of the model is primarily driven by the performance of the fan controller. Third, the referenced approaches required targeted experiments for identification. The framework we propose can be identified primarily using historical undisturbed BAS data. However, in some systems, due to varying design capacity, targeted experiments might be necessary.

## 2. METHODOLOGY

### 2.1 Preliminaries

The supply fan in commercial VAV systems is designed to generate both pressure and airflow to deliver conditioned air to multiple zones. Terminal units regulate airflow by adjusting zone damper positions in response to individual cooling and heating requirements. The interaction between the supply fan and terminal units is the primary consideration for fan design which accounts for aspects such as: size, type, controller, noise, vibration, surge avoidance, and system effects (ASHRAE, 2016). A tool used in design is the *system curve*, which is a graphical representation of the total head loss of a particular system at its design airflow. For turbulent air systems (such as VAV systems), the operation follows the law in Equation 1 closely. By rearranging Equation 1 we obtain Equation 2 describing a quadratic function parametrized by the resistance coefficient. These curves are drawn as functions intersecting the origin in Figure 2a. The resistance coefficient, $R$, is a continuous variable that lumps all of the pressure losses downstream of the fan for a fixed configuration. This term incorporates pressure losses from both static sources (e.g. duct geometry, leakage) and dynamic sources (e.g. terminal dampers). Fan controllers are designed to overcome these pressure losses and maintain constant duct static pressure across all operational system curves. Variable frequency drives (VFD) are commonly used to modulate fan speed, effectively changing the fan performance curves shown in Figure 2a. The intersection between the fan performance curve and the system curve is referred to as the operating point. For a particular fan, determining the operating point is sufficient information to accurately predict power consumption (Stein & Hydeman, 2004).

$$(p_1/p_2) = (Q_1/Q_2)^2 \tag{1}$$

$$p = RQ^2 \tag{2}$$

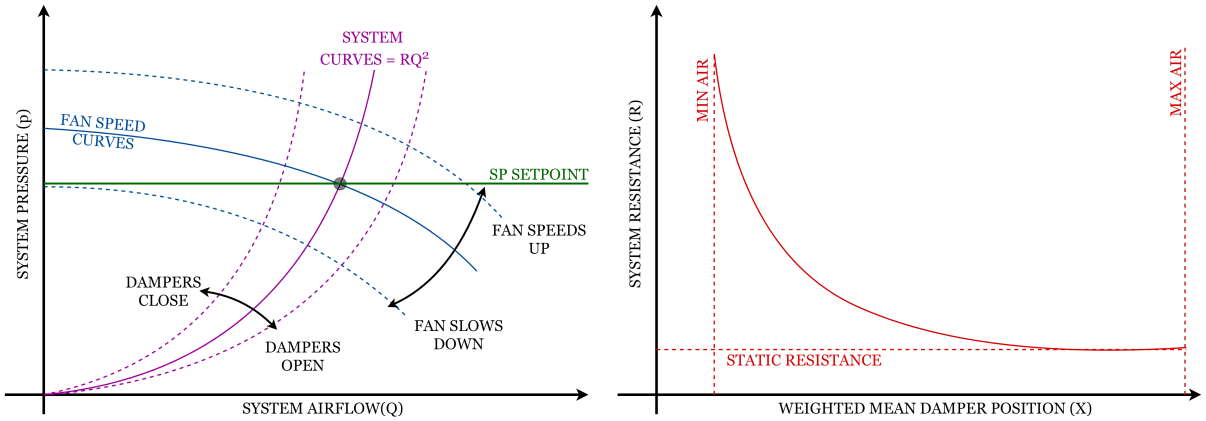


**Figure 2:** (a) Pressure-flow model: Fan Performance and System Curves (b) System resistance model: resistance coefficient vs weighted mean damper position

### 2.2 Model Description

The model approach we seek to develop is based on characterizing and bounding the range of system curves that supply fan is subjected to. Given that dampers are the source of variable resistance, we seek to find a model that maps all feasible configurations of damper positions to a particular system resistance. To do so, we adopt the relation between damper positions ($\boldsymbol{\theta}$) and system resistance ($R$) suggested by (Tukur & Hallinan, 2017). To account for varying VAV box sizes, the damper positions are weighted by their nominal airflow, $\mathbf{w}$. In their work , they implement a dimensionality reduction technique to map the vector of all zone damper positions to a single weighted average value ($X$). We refer

to this relation as the system resistance model shown in Figure 2b. The referenced work leverages this model as a statistical tool to estimate the energy savings of a static pressure reset strategy. We extend the use of this approach to actively control the power consumption of the supply fan. The output of this model can be used in Equation 2 to find the operating point in a pressure-flow balance model of the supply fan which ultimately outputs power. Figure 3 shows the complete modeling framework from damper positions to power. The underlying principle is that for each particular system curve the supply fan will tend towards a known operating point, hence power consumption. This operating point will lie at the intersection between the current system curve and the static pressure setpoint. The dynamics of how the operating point moves are tied to both the changing damper configuration and the performance of the fan controller. One important property is that the system resistance values are bounded by the configurations of minimum and maximum resistance. The lower bound (i.e. minimum resistance) is reached at the point when all dampers are a their most open configuration. This system configuration, otherwise known as the design airflow, is hardly ever reached by most VAV systems by design (Hydeman et al., 2003). The upper bound (i.e. maximum resistance) is reached when all zones are operating at their minimum air setting simultaneously.

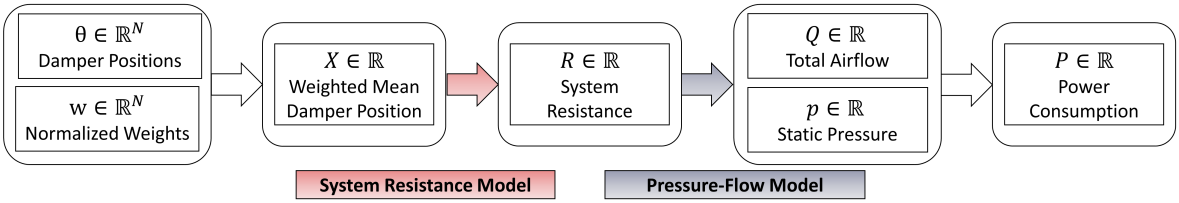


**Figure 3:** Proposed model structure with damper positions as inputs and power consumption as output

Once the two models are calibrated, fan power consumption can be determined for a particular damper configuration. To show how this can be achieved we developed an algorithm to follow a specified power consumption (**P**) for a time horizon ($H$). The desired power consumption is converted to a sequence of system resistances using the pressure-flow model, assuming static pressure setpoint is maintained. The weighted mean damper position ($X$) is obtained by using the system resistance model. Finally, we solve a sequence of optimization problems to determine the damper positions that will output the desired sequence of system resistances. Note that in this simplified case, the optimization problems are in quadratic form having an equality constraint for the weighted mean damper position and a set of inequality constraints to respect each damper's operational limits, $\mathcal{X}$. This simplified algorithm has two important assumptions. The first assumption is that the fan controller ideally maintains the static pressure setpoint. In real systems, this controller is commonly a proportional-integral controller reading static pressure and outputting a speed command to the fan motor. Hence, fluctuations around the static pressure setpoint are expected, but the process variable is expected to reach the setpoint asymptotically. The second assumption is that the zone thermal constraints are not modeled in the action selection process. To provide a complete solution, this approach, which focuses on the mechanical system, needs to be coupled to other constraints that are imposed by a thermal model of the zones.

**Algorithm 1:** Supply Fan Power Control through System Resistance (Damper Positions)

**Input:** Initial weighted damper positions $\mathbf{x}_0$, and desired power consumption **P**.
**Output:** A sequence $\mathbf{x_k^*}\ \forall\ k = 1, \ldots, H$ of commanded damper positions to achieve the desired power deviation **P**.

Solve for $(Q_k^*, \hat{p})$ using $P_k,\ \forall\ k = 1, \ldots, H$ // solve for operating point at static pressure set point
Solve for $R_k^*$ using $({Q_k}^*, \hat{p})\ \forall\ k = 1, \ldots, H$ // solve for sequence of system resistances
Solve for $X_k^*$ using $\hat{R}_k\ \forall\ k = 1, \ldots, H$ // solve for sequence of weighted damper positions
**for** $k \leftarrow 1$ **to** $H$ **do**
    Find $\mathbf{x_k^*}$ that minimizes $||\mathbf{x_k} - \mathbf{x}_0||^2$ // follow predicted damper positions
    **such that:**
    $X_k = \hat{X}_k^*\ \forall\ k = 1, \ldots, H$ // match system resistance
    $\mathbf{x_k} \in \mathcal{X}\ \forall\ k = 1, \ldots, H$ // damper operational limits
**end**
**return** $\mathbf{x_k^*}$

# 3. IMPLEMENTATION

## 3.1 Experimental Calibration

To test the proposed model, we applied an identification process in a three-room testbed located in Carnegie Mellon University's Porter Hall (a 3D render of the testbed is shown in Figure 4). The three zones are served by an exclusive VAV system providing an isolated testbed. The dedicated AHU system is connected to the building automation platform from which remote commands were sent. To validate the model, we covered all combinations of feasible damper positions discretely, and maintained each setting for 5 minutes to allow the system to reach steady state. Note that historical BAS data is also an immediate option as described in Section 4.3. Table 1 shows a summary of the 320 system configurations explored. The nominal airflows used to weigh damper positions for the zones A,B, and C are 0.35, 0.35, and 0.21 $m^3/s$, respectively. During this experiment the fan speed was maintained constantly at 100% to make a clear distinction between system curves. The rooms were completely isolated from users due to possible significant fluctuations in zone temperatures. For this particular system, a weighted mean damper position beyond $X = 0.75$ (i.e. low system resistance) is the maximum value for which the supply fan is capable of maintaining the duct static pressure setpoint ($\hat{p} = 250Pa$). This can be graphically verified by the intersection of the max fan speed curve and the static pressure setpoint in Figure 6. For completeness, we also recorded data points beyond this setting to validate the asymptotic portion of the model where the static losses dominate the change in system resistance. Figure 5 shows the results from the set of experiments previously described. Note that the system resistance parameter was normalized by its maximum value for clarity. The key takeaway from Figure 5 is that it validates the dimensionality reduction technique from $\boldsymbol{\theta} \in \mathbb{R}^N$ to $X \in \mathbb{R}$. Additionally, we fitted a third order polynomial to the feasible range of the model after uniformly sampling the data . The model choice was made to simply select a low-order continuous model that shows a good fit (i.e. $R^2 = 98.5\%$).

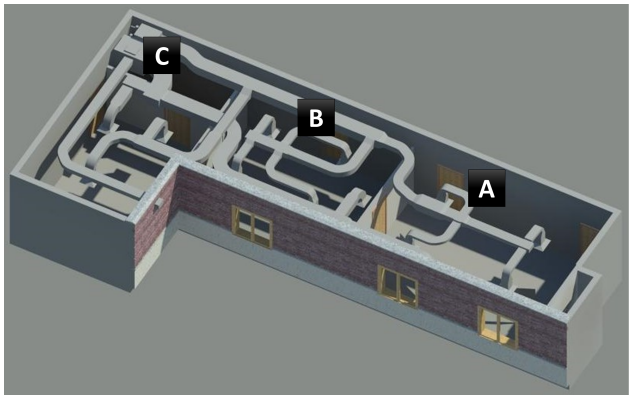


**Figure 4:** Porter Hall: 3-zone VAV Experimental Testbed

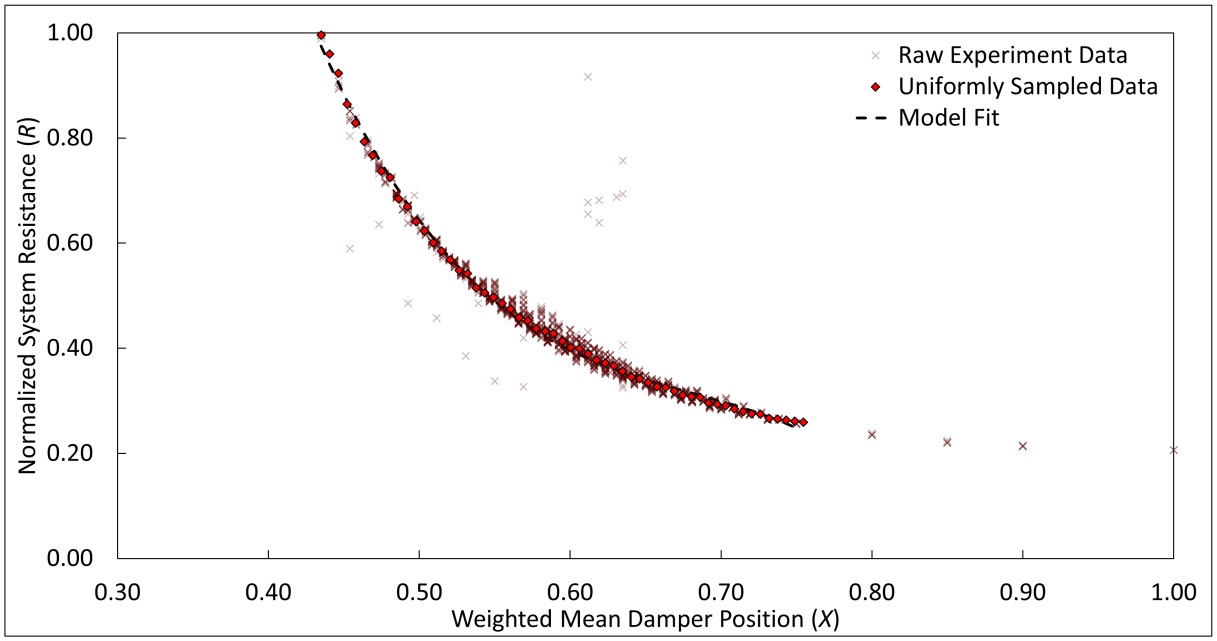


**Figure 5:** Experimental System Resistance Model from Porter Hall Testbed

**Table 1:** Set of tested damper positions for identification experiments

| ZONE | 1 | 2 | 3 | 4 | 5 | 6 | ... | 315 | 316 | 317 | 318 | 319 | 320 |
|---|---|---|---|---|---|---|---|---|---|---|---|---|---|
| A | 0.40 | 0.40 | 0.40 | 0.40 | 0.40 | 0.40 | ... | 0.75 | 0.75 | 0.75 | 0.75 | 0.75 | 0.75 |
| B | 0.40 | 0.40 | 0.40 | 0.40 | 0.40 | 0.45 | ... | 0.70 | 0.75 | 0.75 | 0.75 | 0.75 | 0.75 |
| C | 0.55 | 0.60 | 0.65 | 0.70 | 0.75 | 0.40 | ... | 0.75 | 0.55 | 0.60 | 0.65 | 0.70 | 0.75 |

A second set of experiments were performed to identify the fan's pressure-flow characteristics. Although the manufacturer provided performance curves can be used, these curves are generated using standardized laboratory conditions (ASHRAE, 2016). Hence, they do not include the performance of the system under the installed conditions, which is in most cases different than the design conditions. In this case, 8 characteristic system curves were tested for varying fan speeds to create the pressure-flow model. Similar to the system resistance model, this set of experiments are performed to support the validity of the model. For each system configuration the fan speed ($\omega$) was varied in steps of 10%. This set of curves included both the minimum and maximum system resistance curves encountered by this unit. The system curves were fitted with second-order polynomials closely following the expected theoretical results from Equation 2 (i.e. $R^2 > 0.99$). A plot of these results is shown in Figure 6. Interestingly, the 8 system curves from the second experiment can also be used to build the system resistance model, yielding virtually identical model fit to the one shown in Figure 5. For this unit, the combination of the model in Figure 5 and Figure 6 bound and characterize the available demand flexibility of the air distribution system.

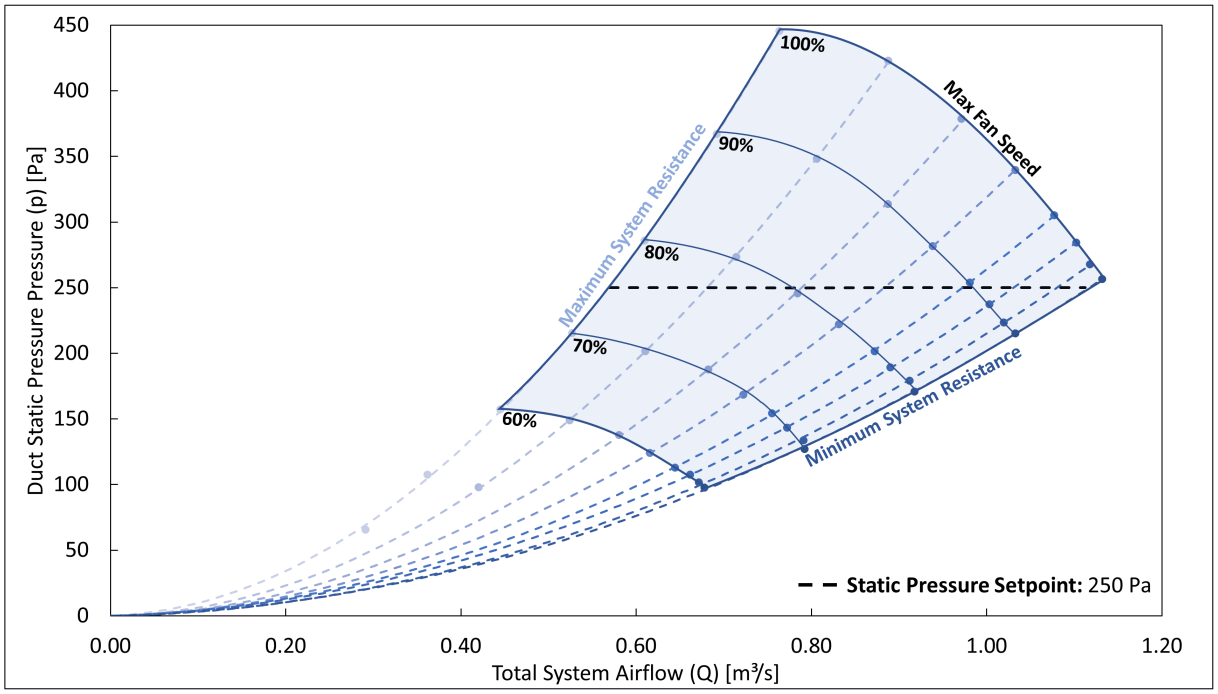


**Figure 6:** Experimental Fan Performance and System Curves to form the Pressure-Flow Model for Porter Hall Testbed

### 3.2 Simulation Results

To test the control algorithm on a dynamic setting, we created a model of the experimental setting using the Modelica Buildings Library (Wetter, Zuo, Nouidui, & Pang, 2014). The simulation model is based of a VAV system example the library includes using the control sequence where the supply fan is regulated based on the duct static pressure. Using the experimental data, the model of the HVAC system and the three thermal zones was created. We first build an offline system resistance model using simulated data gathered from a week of undisturbed operation. Similarly, the fan pressure-flow model is calibrated with the experimental results. Then we selected a power deviation trajectory for the supply fan to follow. In this setting we used PJM's RegA test signal to use a low frequency signal to follow for an hour (Macdonald et al., 2014). The choice of signal is based on selecting a standard power deviation signal rather than suggesting the exclusive use for this model for frequency regulation. We also selected a arbitrarily predicted trajectory

for the three dampers over the one hour horizon, which simulated dynamic cooling demand. Figure 7 shows the results of this simulation. The left pane of the figure shows the predicted and actual damper positions for the three zones as well as the damper operational limits. This figure shows that the control algorithm follows closely the predicted damper positions. All zone dampers respect the operational limits for the entire event. The right pane shows the results of the system resistance model for this simulated unit. Although not included in the optimization algorithm, the temperature deviations in the three zones are less than 0.50°C. This continues to reinforce the property that zones have the thermal capacity to not experience significant temperature deviations for fast changes in airflow. The results comparing the desired power deviation and measured power deviation are not shown as they are almost identical meaning that the algorithm accurately tracked the demand flexibility event. However, the simulation environment reflects an idealized HVAC system and further studies are needed to validate the accuracy of this approach in an experimental setting.

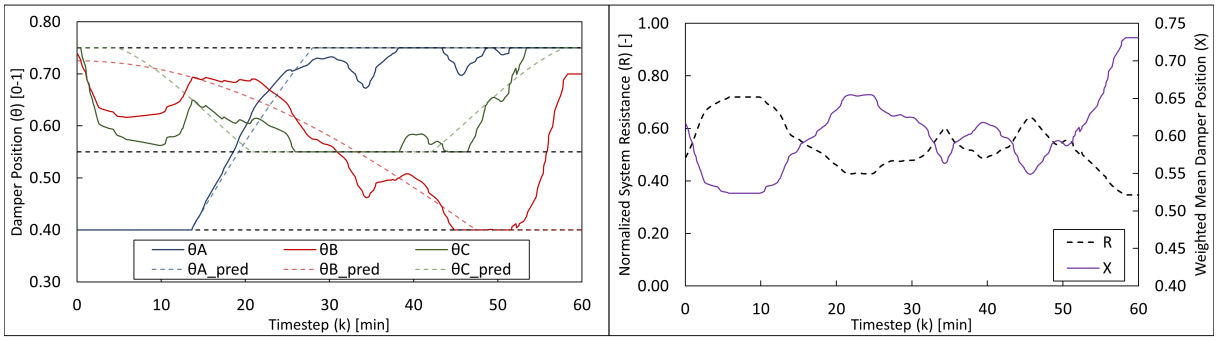


**Figure 7:** Simulation results (a) damper positions for the three zones denoted as A,B,C in the figure (b) system resistance model results for demand flexibility event

## 4. RESULTS AND DISCUSSIONS

### 4.1 System Bounds

An important property of this modeling approach is to quantitatively define the bounds on which an installed system would be subjected to, independent of zone-level control input. This, in turn, defines the available range power can be actuated for a particular system. As VAV systems develop from the original design intent to operation, intermediate choices lead to unique operational range across buildings. These bounds can be observed in the limits of the system resistance model. For example, for the Porter unit, the extreme system resistance values occur within the range $0.44 \leq X \leq 0.75$. For comparison, we show a different 5-zone VAV system, referred to as Gate (see Figure 8), whose system bounds occur within the range $0.10 \leq X \leq 0.30$. This range is unique to the control sequence and capacity each installed system and can be used to qualify certain buildings for different types of grid services. For example, the normal operation of the Porter unit shows that it runs at minimum air over 90% of the time, indicating an over-designed capacity. This observation shows that, although the zones inherently have thermal capacity, this system is currently not suitable for participating in load shedding reliability-based services such as contingency reserves. On the other hand, the Gate unit nominally operates across its available range, as depicted historical data in Figure 8. For this unit, the range derived from this modeling structure, is significantly lower than the range that would be derived form using airflow setpoint as a control variable. Hence, airflow setpoint control would misrepresent the demand flexibility of the Gate system.

### 4.2 Control Performance

In a complementary study of 35+ AHUs, we analyzed the qualification of airflow as a proxy for dynamic fan power control in VAV systems. Due to the imperfect operation of control loops and controllers, a simplified polynomial relation between airflow setpoints and power does not show high accuracy in predicting power consumption. This is likely because changes in airflow setpoint are dependent on the zone airflow controllers and are subject to latency in reaching the fan controller at the AHU level. Note that for certain applications, such as energy efficiency and unmeasured load shedding, the airflow-to-power assumption might be sufficient. However, more demanding grid services require sequential control inputs, sometimes in a timescale of minutes, that accurately shape power consumption. An important property of our modeling approach, and others that control damper position, is that there are no intermediate control loops that distort or delay the effect of control inputs. This means the effect of dynamic control inputs on fan

power are primarily explained by the performance of the fan controller. For example, the Porter unit has a poorly tuned fan controller making it respond slowly to changes in static pressure. The performance of this individual controller restricts the use of this unit for grid services that require fast changes in power consumption. More importantly, the limitation can be measured and pinpointed to the parameters of the proportional integral (PI) fan controller. Under the assumptions of existing modeling approaches, this limitation would not be highlighted causing to misrepresent the demand flexibility of the Porter unit.

### 4.3 Generalizability

Another property we wanted to hold with the presented modeling approach is the ability to identify the model with undisturbed historical BAS data. In the complementary study referenced in Section 4.2, we find that in most systems the recorded data covers the minimum and maximum resistance damper configuration. The Gate unit, in Figure 8, shows how historical BAS data can be used to fully characterize the system resistance model. One important aspect to note is that although the Gate system resistance model was built using historical data, there was significant preprocessing before raw data can be used. For reference, Figure 8 only shows 20% of the raw data collected for a 3 month period at a 1 min resolution. This is because a large portion of the raw data was excluded because it was generated from modes outside the expected operation of the unit. For example, portions of the data showed the static pressure drop significantly below the setpoint, because the fan capacity was not able to meet the airflow requests from the VAV terminal dampers. This is a evidence of a mechanical system limitation that would not be captured by using airflow control at the zone level. Further work needs to be done to design a method that processes raw BAS data to build models, such as the one presented, using domain informed decisions based on the expected behavior of the system.

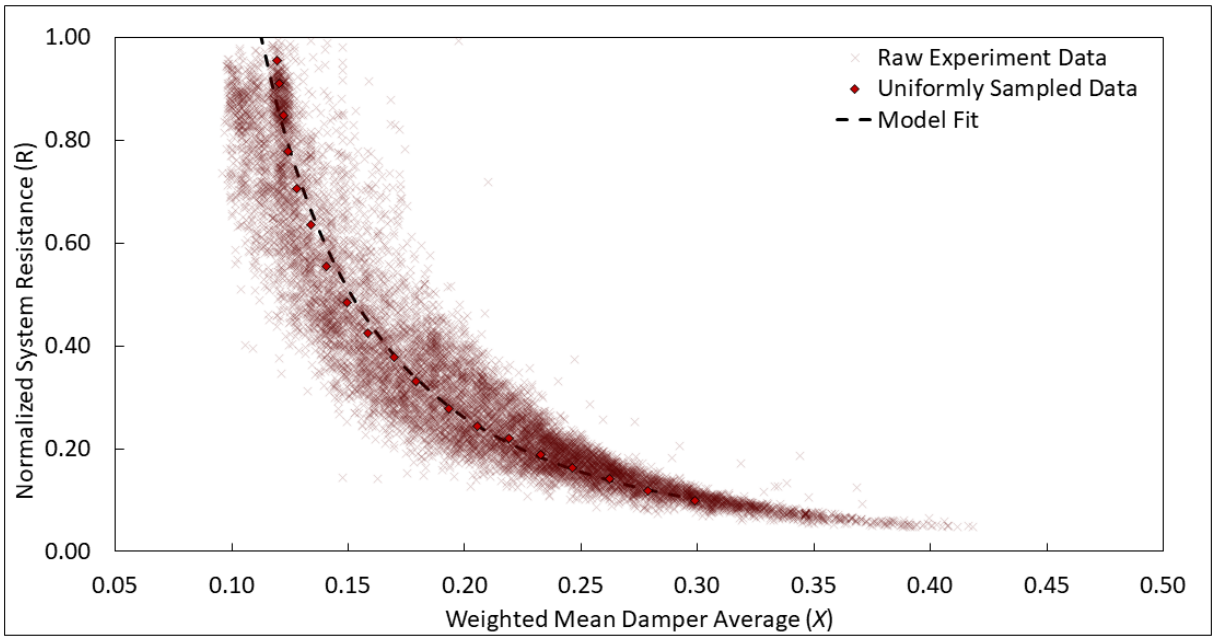


**Figure 8:** System Resistance Model for Gate Unit (Generated from undisturbed historical BAS data)

## 5. CONCLUSIONS

We presented a modeling approach to characterize the demand flexibility of the supply fan in VAV systems. The model maps all terminal zone damper configurations to a particular system resistance connected to a pressure-flow model of the supply fan to control its power consumption. Using this framework, the operational range of an existing unit can be quantitatively bounded by the minimum and maximum resistances the fan operation is subjected to. A control algorithm was proposed that leverages this model structure taking in a desired power deviation and outputting a sequence of damper configurations to achieve it. There are various avenues for continued work. We plan to extend and improve this modeling approach through experimental validation in different units. Another extension is to include data from a dedicated fan power meter to complete the pressure-flow model. This would include the effect of varying efficiencies in fan performance curves. We also plan to improve and extend the control algorithm we presented to include the zone

thermal dynamics as constraints and incorporate predictive capabilities. Another avenue of investigation is the use of this approach, to extend compatibility with more advanced control sequences with trim & respond logic such as the ASHRAE Guideline 36 (ASHRAE, 2018). Given that this approach consists of relatively simple relations, we expect it can serve as a complementary model to other methods that focus on thermal comfort. Finally, another line we are exploring is the use of the theoretical foundations of this model for fault detection and diagnosis applications.

## NOMENCLATURE

| | | |
|---|---|---|
| $\boldsymbol{\theta} = \{\theta_1, \theta_2, \ldots, \theta_N\}$ | zone damper positions | (-) |
| $\mathbf{w} = \{w_1, w_2, \ldots, w_N\}$ | VAV box nominal airflow | $(m^3/s)$ |
| $\mathbf{x} = \{x_1, x_2, \ldots, x_N\}$ | weighted damper positions | (-) |
| $\mathbf{q} = \{q_1, q_2, \ldots, q_N\}$ | zone airflow | $(m^3/s)$ |
| $\mathbf{P} = \{P_1, P_2, \ldots, P_H\}$ | power consumption sequence | (kW) |
| $\mathcal{X} \coloneqq \{\ \mathbf{x}\ \vert \underline{\mathbf{x}} \leq \mathbf{x} \leq \bar{\mathbf{x}}\}$ | feasible damper positions | (-) |
| $X$ | weighted mean damper position | (-) |
| $R$ | system resistance coefficient | $(Pa/(m^3/s)^2)$ |
| $Q$ | system total airflow | $(m^3/s)$ |
| $p$ | system static pressure | $(Pa)$ |

* hat (ˆ) notation used to denote a setpoint

**Subscript**

| | |
|---|---|
| N | number of zones |
| H | time horizon |
| k | timesteps |

## REFERENCES


Adetola, V., Lin, F., Adetola, V., Lin, F., Yuan, S., & Reeve, H. (2018). Building Flexibility Estimation and Control for Grid Ancillary Services. In *International high performance buildings conference.*

ASHRAE. (2016). *2016 ASHRAE Handbook - Fundamentals (SI Edition).* American Society of Heating, Refrigerating and Air-Conditioning Engineers.

ASHRAE. (2018). *Guideline 36-2018 – High-Performance Sequences of Operation for HVAC Systems* (No. May). American Society of Heating, Refrigerating and Air-Conditioning Engineers.

Blum, D. H., & Norford, L. K. (2014, 11). Dynamic simulation and analysis of ancillary service demand response strategies for variable air volume HVAC systems. *HVAC and R Research*, *20*(8), 908–921. doi: 10.1080/10789669.2014.958975

Dong, J., Im, P., Huang, S., Chen, Y., Münk, J., & Kuruganti, T. (2019). Development and calibration of an online energy model for AHU fan. *ASHRAE Transactions*, *125*, 341–349.

Goddard, G., Klose, J., & Backhaus, S. (2014, 7). Model Development and Identification for Fast Demand Response in Commercial HVAC Systems. *IEEE Transactions on Smart Grid*, *5*(4), 2084–2092. Retrieved from `http://ieeexplore.ieee.org/lpdocs/epic03/wrapper.htm?arnumber=6839121` doi: 10.1109/TSG.2014.2312430

Hydeman, M. M., Taylor, S. T., Stein, J., Kolderup, E., & Hong, T. (2003). *Advanced Variable Air Volume System Design Guide.*

Jing, G., Cai, W., Zhang, X., Cui, C., Yin, X., & Xian, H. (2019). Modeling, air balancing and optimal pressure setpoint selection for the ventilation system with minimized energy consumption. *Applied Energy*, *236*(September 2018), 574–589. Retrieved from `https://doi.org/10.1016/j.apenergy.2018.12.026` doi: 10.1016/j.apenergy.2018.12.026

Kathirgamanathan, A., De Rosa, M., Mangina, E., & Finn, D. P. (2021). Data-driven predictive control for unlocking building energy flexibility: A review. *Renewable and Sustainable Energy Reviews*, *135*(January 2020), 110120. Retrieved from `https://doi.org/10.1016/j.rser.2020.110120` doi: 10.1016/j.rser.2020.110120

Keskar, A., Anderson, D., Johnson, J. X., Hiskens, I. A., & Mathieu, J. L. (2019). Do commercial buildings become less efficient when they provide grid ancillary services? *Energy Efficiency*. doi: 10.1007/s12053-019-09787-x

Macdonald, J., Kiliccote, S., Boch, J., Chen, J., & Nawy, R. (2014). Commercial Building Loads Providing Ancillary Services in PJM. *2014 ACEEE Summer Study on Energy Efficiency in Buildings*, 192–206.

MacDonald, J. S., Vrettos, E., & Callaway, D. S. (2020). A Critical Exploration of the Efficiency Impacts of Demand

Response From HVAC in Commercial Buildings. *Proceedings of the IEEE*, 1–17. Retrieved from https://ieeexplore.ieee.org/document/9143166/ doi: 10.1109/JPROC.2020.3006804

Neukomm, M., Nubbe, V., & Fares, R. (2019, 4). *Grid-Interactive Efficient Buildings* (Tech. Rep. No. April). EERE Publication and Product Library. Retrieved from http://www.osti.gov/servlets/purl/1508212/ doi: 10.2172/1508212

Raisoni, R., Raman, N. S., Barooah, P., Munk, J. D., & Im, P. (2018). A Control-Oriented Dynamic Model of Air Flow in a Single Duct HVAC System. In *5th international high performance buildings conference at purdue* (pp. 1–10).

Roth, A., & Reyna, J. (2020, 11). *Innovations in Building Energy Modeling: Research and Development Opportunities for Emerging Technologies* (Tech. Rep. No. November). Golden, CO (United States): National Renewable Energy Laboratory (NREL). Retrieved from https://www.osti.gov/servlets/purl/1710155/ doi: 10.2172/1710155

Stein, J., & Hydeman, M. M. (2004). Development and testing of the characteristic curve fan model. *2004 Winter Meeting - Technical and Symposium Papers, American Society of Heating, Refrigerating and Air-Conditioning Engineers*, 303–312.

Tukur, A., & Hallinan, K. P. (2017). Statistically informed static pressure control in multiple-zone VAV systems. *Energy and Buildings*, *135*, 244–252. Retrieved from http://dx.doi.org/10.1016/j.enbuild.2016.11.032 doi: 10.1016/j.enbuild.2016.11.032

Ulbig, A., & Andersson, G. (2015). Analyzing operational flexibility of electric power systems. *International Journal of Electrical Power and Energy Systems*, *72*, 155–164. Retrieved from http://dx.doi.org/10.1016/j.ijepes.2015.02.028 doi: 10.1016/j.ijepes.2015.02.028

Wang, J., Huang, S., Wu, D., & Lu, N. (2020). Operating a Commercial Building HVAC Load as a Virtual Battery through Airflow Control. *IEEE Transactions on Sustainable Energy*, *3029*(c), 1–1. doi: 10.1109/tste.2020.2988513

Wetter, M., Zuo, W., Nouidui, T. S., & Pang, X. (2014, 7). Modelica Buildings library. *Journal of Building Performance Simulation*, *7*(4), 253–270. Retrieved from http://www.tandfonline.com/doi/abs/10.1080/19401493.2013.765506 doi: 10.1080/19401493.2013.765506

Yin, R., Kiliccote, S., & Piette, M. A. (2016, 7). Linking measurements and models in commercial buildings: A case study for model calibration and demand response strategy evaluation. *Energy and Buildings*, *124*, 222–235. Retrieved from http://dx.doi.org/10.1016/j.enbuild.2015.10.042 doi: 10.1016/j.enbuild.2015.10.042

## ACKNOWLEDGMENT

The authors would like to gratefully acknowledge the support provided by the Pennsylvania Infrastructure Technology Alliance (PITA). The authors are also thankful for the assistance in data and building automation control access to the Facilities Management and Campus Services team at Carnegie Mellon University.